

Sphericity and morphology of smoke particles from biomass burning in Brazil

J. Vanderlei Martins,^{1,2} Peter V. Hobbs,² Ray E. Weiss,³ and Paulo Artaxo¹

Abstract. The degree of nonsphericity of smoke particles from biomass burning in Brazil was measured aboard the University of Washington C-131A aircraft during the Smoke, Clouds, and Radiation–Brazil (SCAR–B) project for several regions, types of fuel, and combustion. The nonsphericity (α_o) of the particles was obtained from electrooptical light-scattering measurements, using an aerosol asymmetry analyzer, and from scanning electron microscopy (SEM) images of the particles. The electrooptical measurements provide a measure of the nonsphericity based on the difference between the light scattering coefficient for aligned and randomly oriented particles. The SEM photographs provide information on the geometric shapes of the particles. The maximum value of α_o obtained during the SCAR-B for biomass burning in Brazil was below 13%. The degree of nonsphericity of the particles is shown to be related to the combustion efficiency, the mass absorption efficiency, and the fraction of black carbon to total particle mass. It is concluded after smoke particles from biomass burning in Brazil have been in the atmosphere for more than about 1 hour that the spherical approximation (and therefore Mie theory) is reasonably valid for estimating the physical and optical properties of the particles.

1. Introduction

Radiative transfer calculations for aerosols generally assume that the particles are spherical. For example, this assumption has been used for estimating direct radiative forcing by smoke particles from biomass burning [Penner *et al.*, 1992; Hobbs *et al.*, 1997] and for deriving aerosol properties from remote sensing measurements [Kaufman *et al.*, 1990, 1997]. Mie calculations apply strictly only to spherical and homogeneous (or in some cases, spherically concentric) particles. However, because of its relative simplicity, Mie theory is often used to estimate the scattering and absorption properties of nonspherical particles. Two widely used approaches employ volume or surface area equivalent spheres for describing nonspherical particles [Chylek and Ramaswamy, 1982]. Although this approach may be reasonable in some cases, recent studies have shown that it can produce misleading results in the retrieval of aerosol physical properties using remote sensing techniques [Kahn *et al.*, 1997; Mishchenko *et al.*, 1997; West *et al.*, 1997].

Particles from biomass burning are generally composed of a mixture of spherical and nonspherical particles and chain aggregates. The morphology and structure of smoke particles from biomass burning are determined by the type of fuel, the phase of combustion, and the age of the smoke. The structure, composition, and size of smoke particles change rapidly with aging, with very nonspherical and fluffy aggregates becoming more compacted and increasingly spherical with age [Hallet *et al.*, 1989; Reid and Hobbs, this issue]. Large fluffy cluster aggregates are generally found only near the source, particularly

for flaming-phase combustion, which suggests that particle compaction occurs in a relatively short time (likely, few hours) after release from a biomass fire.

The phase of combustion (flaming or smoldering) is related to the combustion efficiency (CE) and the ratio of black carbon (BC) to the total particle mass (TPM) [Lobert and Warnatz, 1993; Yamasoe, 1994; Martins *et al.*, 1996]. High combustion efficiencies (CE > 0.9) are associated with flaming combustion and low combustion efficiencies with smoldering combustion [Ward *et al.*, 1992]. Similarly, high values of BC/TPM are generally associated with flaming-phase combustion and low values with smoldering combustion. Ward *et al.* [1992] found that most of the smoke produced by cerrado (Brazilian savanna) fires came from flaming combustion and most of the smoke in the rain forest regions from smoldering combustion.

The geometric shapes of aerosol particles may be measured by scanning or transmission electron microscopy. Unfortunately, the relationship between the geometric shape and the optical properties of a particle is not straightforward. Also, the effects of the nonsphericity of a particle on its optical properties depend not only on the shape of the particle but also on its size. Therefore in the case of smoke particles the large variability in their size and shape produces additional difficulties in determining their optical properties. Electrooptical nephelometry provides measurements of the effects of both particle shape and size on light scattering [Kapustin *et al.*, 1980; Cheng *et al.*, 1991]. In this technique, measurements of light scattering are used to detect nonspherical particles by comparing the amount of light they scatter when uniformly oriented to that which they scatter when randomly oriented.

In this paper, we use both electrooptical nephelometry and electron microscopy to provide information on the degree of nonsphericity of smoke particles from various types of biomass burning and smoke of various ages in Brazil. The measurements were obtained aboard the University of Washington (UW) C-131A research aircraft as part of the Smoke, Cloud, and Radiation–Brazil (SCAR–B) project.

¹Instituto de Física, Universidade de São Paulo, São Paulo, Brazil.

²Department of Atmospheric Sciences, University of Washington, Seattle.

³Radianc Research, Inc., Seattle, Washington.

2. Methodology

Scanning electron microscopy (SEM) photographs were taken of Nuclepore filters on which smoke particles were collected on the UW aircraft. An isokinetic inlet system was used, with a cutoff diameter of about 4–5 μm . After sampling, the Nuclepore filters were weighed on a microbalance and submitted to optical reflectance analysis. A small piece of each filter was then cut and coated with a thin layer of gold prior to SEM analysis. Several photographs of each coated sample were taken in a 25 kV JEOL scanning electron microscope at several magnifications. The SEM photographs were used to determine qualitatively the shapes and sizes of the smoke particles. Samples containing particles with similar morphology and size (small isolated spheres, closed cluster aggregates, small open aggregates, and large chain aggregates) were grouped for comparison with other measurements (electrooptical, absorption coefficient, and combustion efficiency). In some cases it was possible to distinguish between “young” and “aged” smoke particles. The expressions young and aged will be used, respectively, for particles likely collected up to 1 hour after being released from the fire and particles collected more than 1 hour (often days or even weeks) after being released from the combustion zone. Particles in regional hazes will also be described as aged.

At the same time as the filters were exposed to the smoke, measurements of the degree of nonsphericity of the particles were obtained using an electrooptical nephelometer called the aerosol asymmetry analyzer (A^3) [Weiss *et al.*, 1992]. The asymmetry of a particle is evaluated through the difference in the integrated light-scattering coefficient for the randomly oriented particles and for the particles oriented along an applied electrical field. The electric field oscillates, changing its sign and following a square wave function with a frequency of 50 Hz, allowing fast online measurements of the asymmetry of the particles. The A^3 uses a He-Ne laser beam as a light source and integrates the scattered light from 7° to 183° . The electrooptical response (α_o), also referred to as the “nonsphericity parameter,” is defined as

$$\alpha_o (\%) = 100(I_I - I_0)I_0$$

where I_I is the intensity of light scattering for (oriented) particles in the presence of the electric field, and I_0 is the intensity of light scattering for particles randomly oriented in the absence of the electric field. The value of α_o is inversely dependent on the sphericity of the particles; thus spherically symmetrical particles produce lower values of α_o than nonspherical particles.

The relationship between α_o and the shape of the particles is not unique, because α_o depends upon the sizes of the particles as well as their shapes. Also, *Mishchenko et al.* [1997] shows that for absorbing aerosols the effect of the nonsphericity on light scattering is smaller than for nonabsorbing particles.

In addition to the effects of particle shape on light scattering, it is important to understand the effect of nonsphericity on other optical properties (such as light absorption and phase function). Studies with several forms of nonspherical Chebyshev particles (theoretical nonspherical particles with several different forms, produced by rotating functions described by Chebyshev polynomials) by *Mugnai and Wiscombe* [1986] and *Chylek and Ramaswamy* [1982] indicate that on average, for size parameters ($\alpha = 2\pi r/\lambda$) smaller than 5 there is very little variation in light scattering, absorption, single-scattering al-

bedo, hemispheric backscattered fraction for isotropic incident radiation (as defined by *Wiscombe and Grams* [1976]), and the asymmetry factor, between nonspherical and equivalent volume spherical particles (less than 2% in most cases). For solar wavelengths, most smoke particles have a size parameter below 5; so the equivalent sphere approximation to estimate the integral optical properties should be good. On the other hand, *Mugnai and Wiscombe* [1989] and *Wiscombe and Mugnai* [1988] found that for the same type of Chebyshev particles the angular scattering was very sensitive to the shape of the particle, reaching up to 100% difference for certain backscattering angles as compared to spherical particles. The standard deviation of the mean scattered intensity may be up to about 30% (for size parameters between 1 and 5) for particles with an average deformation of only about 10% and several particle shapes [*Mugnai and Wiscombe*, 1989].

The mass absorption efficiency was derived from absorption measurements with the optical reflectance technique and aerosol mass concentration measurements from gravimetric analysis of the Nuclepore filters. The optical reflectance technique was calibrated using the Monarch 71 standard for black carbon, and it was intercalibrated with the optical extinction cell and several other methods for measuring light absorption aboard the C-131A aircraft [*Reid et al.*, this issue]. The intercalibration with the extinction cell showed that the optical reflectance technique produced good measurements (a correlation coefficient r of 0.9 between optical reflectance and extinction cell) of light absorption by particles from biomass burning in Brazil [*Reid et al.*, this issue].

An important difference between the A^3 and the SEM observations is that the A^3 measures partially dried particles (due to warming as they enter the aircraft), which may contain some water. The SEM instrument operates in a high vacuum completely drying the particles and, possibly, evaporating some volatile compounds. Thus the SEM processing may lead to less spherical particles than the A^3 .

3. Results

Figure 1 shows individual measurements of α_o provided by the A^3 for each of the regions in Brazil sampled from the C-131A aircraft. Since the A^3 technique requires relatively high concentrations of particles, most of the measurements were made in smoke plumes relatively close to the fires. Smoke particles from Marabá had lower values of α_o than those from the other three regions studied in Brazil. The values of α_o for Marabá ranged from near zero to over 10%, with the majority of the α_o values below 4%. Figures 2a–2g show a sequence of SEM photographs obtained in parallel with the A^3 measurements for various types of smoke particles, combustion efficiencies, and BC/TPM values. In these photographs the particles appear black and the filter pores as white circles ($\sim 0.35 \mu\text{m}$ diameter). The SEM pictures from Marabá also show a large relative number of spherical particles. Most of the filters from Marabá showed very spherical and compacted particles, similar to those shown in Figure 2g, which are normally associated with smoldering combustion. These results are consistent with the predominant type of vegetation around Marabá (rain forest), which produces large amounts of smoldering combustion and spherical-like particles [*Ward et al.*, 1992; *Yamasoe*, 1994; *Martins et al.*, 1996].

The α_o values varied from less than 1% to about 5% for Brasília, 0 to greater than 12% for Cuiabá, and 0.1 to 11% for

Porto Velho (Figure 1). Samples from Porto Velho showed the clearest separation between symmetrical and nonspherical particles, with a well-defined group of particles with α_o values below 2% and another group with higher values of α_o (Figure 1).

3.1. Samples Collected Near the Combustion Zone

Figures 2a and 2b show SEM photographs at two different magnifications for a sample collected near Porto Velho in smoke recently released from the flaming phase combustion (CE = 0.98) of a forest fire. The sample is composed of very small nonspherical particles and large (~10 μm) chain aggregates. Both of these particle types were likely formed by the agglomeration of small, spherical-like particles. The A^3 results for this sample yielded one of the highest values for α_o measured by us in SCAR-B (about 11%). Figure 2c shows a sample from a grass fire near Brasília, which also originated from flaming-phase combustion (CE = 0.95). The particles are similar to those shown in Figure 2b but with no large aggregates such as those shown in Figure 2a; the α_o value was about 4%. Figures 2d and 2e show large ash particles and the remains of vegetation (~5–20 μm), small spherical particles, and chain aggregates collected near Porto Velho. Combustion efficiency measurements are not available for this case; α_o was about 1.5%. Figures 2f and 2g are representative of particles produced by smoldering combustion of a forested area near Ma-

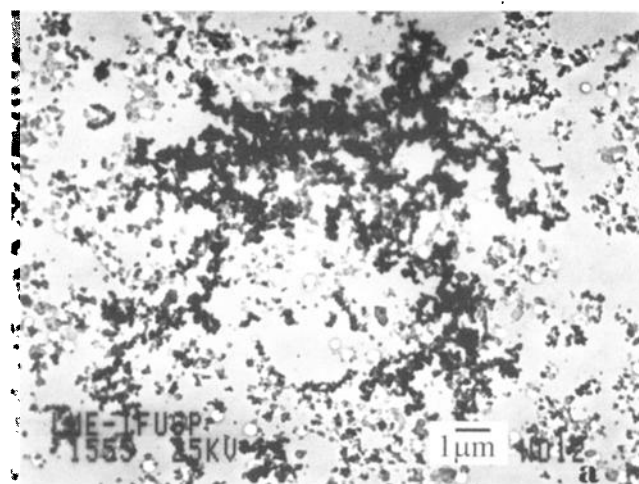


Figure 2. Scanning electron microscopy (SEM) photographs of smoke particles. (a) Sample collected in Porto Velho in flaming combustion of forest fuel showing a very large (~10 μm) cluster aggregate with an open structure composed of thousands of small (~0.05 μm) spherical particles. The combustion efficiency (CE) was 0.98, and the nonsphericity parameter (α_o) from the A^3 was 11% (filter WN 59). (b) Same sample as Figure 1a (filter WN 59) showing smaller particles at higher magnification. Many individual submicrometer particles and small chain aggregates, characteristics of flaming combustion, can be seen. Although the individual particles are nearly spherical, most of the chain aggregates are highly nonspherical. (c) Nuclepore filter (WN 08) exposed to smoke from a cerrado fire near Brasília. The particles are characteristic of flaming-phase combustion (CE = 0.95, α_o = 4%). All the smoke particles collected in this region had similar characteristics. (d) Nuclepore filter (WN 58) exposed in Porto Velho. The sample contains large (~10 μm) nonspherical particles and small (< 1 μm) spherical particles (see Figure 1e). The nonsphericity parameter (α_o) was about 1.5%. This low value of α_o shows that despite the presence of some large nonspherical particles, the total light scattering was dominated by the more numerous, smaller and more symmetrical particles. (e) Same sample as Figure 1d (filter WN 58) but at higher magnification. The sample contains a mixture of small spherical particles and small chain aggregates (α_o = 1.5%). (f) Mostly spherical particles mixed with some small and very compressed aggregates (filter WN 76). The relatively low combustion efficiency (CE = 0.88), field observations during the sampling, and the characteristics of the particles shown here, indicate mixed particles dominated by smoldering-phase aerosols. The nonsphericity parameter was low (α_o = 1%). (g) Nuclepore filter (WN 81) exposed in smoke from smoldering phase combustion near Marabá. Most of the particles are nearly spherical and there are no soot clusters (CE = 0.80, α_o = 1%).

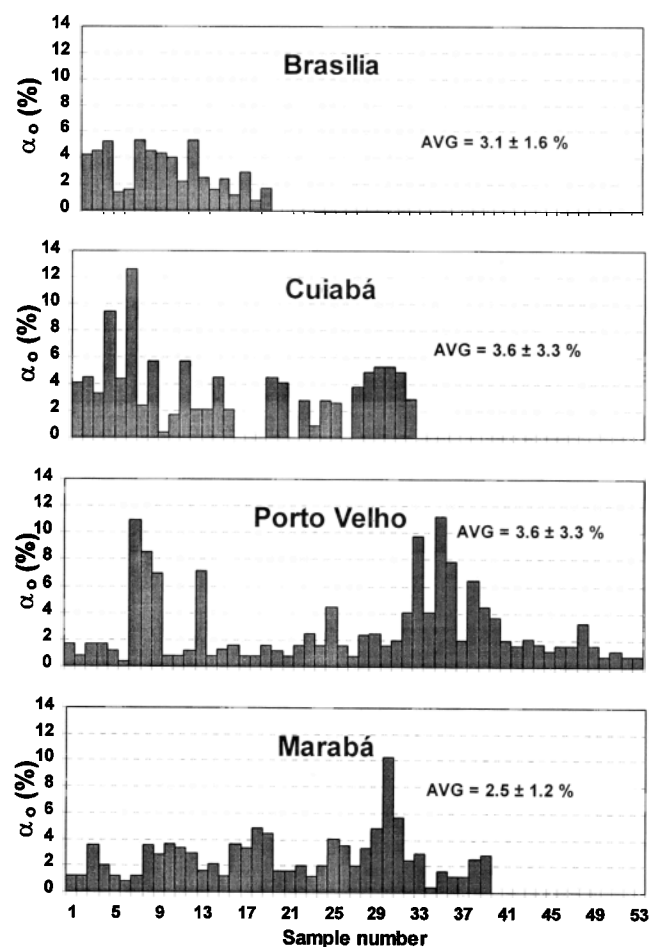


Figure 1. Measurements of the nonsphericity parameter (α_o) of smoke particles from four regions in Brazil obtained from the A^3 instrument aboard the University of Washington C-131A aircraft in SCAR-B.

rabá. Figure 2g, which corresponds to the lowest combustion efficiency measured (CE = 0.80), shows fairly spherical particles smaller than 1 μm diameter, with no aggregates or large particles (α_o = 0.8%). Figure 2f, which had a CE of 0.88, shows spherical homogeneous particles and several spherical-like compact aggregates (α_o about 1%). The degree of sphericity qualitatively observed in the SEM photographs agree well with the value of α_o measured with the A^3 .

Flaming combustion produced high concentrations of very small soot particles (~0.05 μm diameter), which were conducive to the formation of particle clusters. Such clusters can be submicron to tens of micrometers in size and they assume

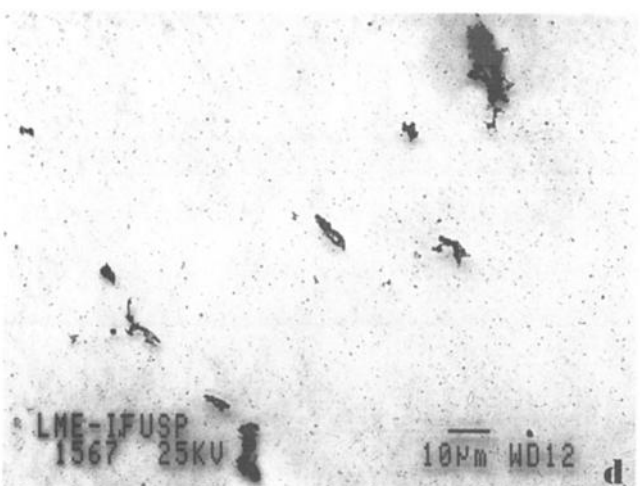
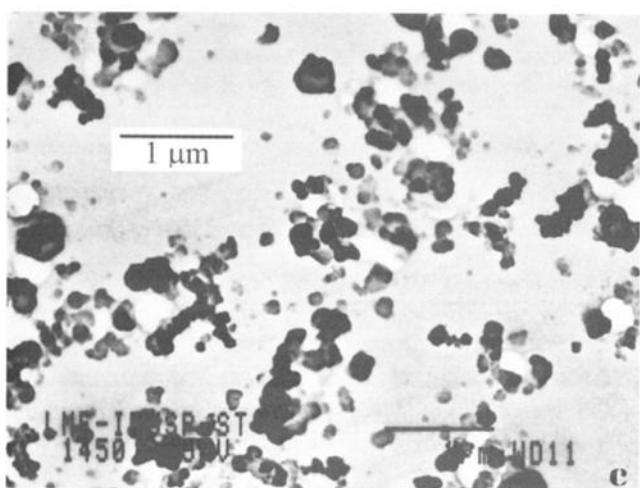
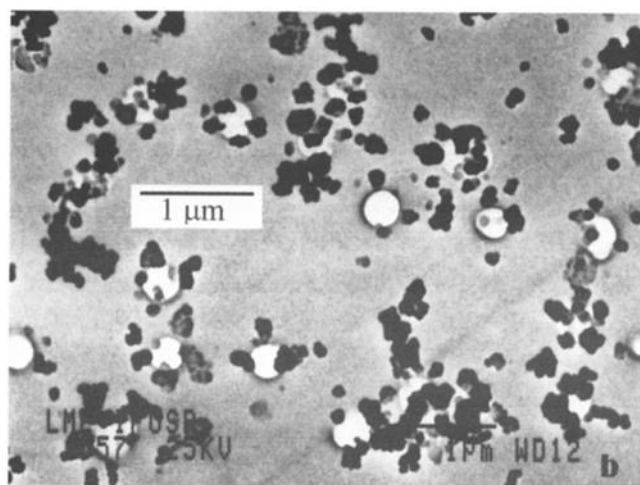


Figure 2. (continued).

various shapes (Figures 2a, 2b, and 2c). Young clusters generally consist of large open structures with very low density (Figure 2a). After aging in the atmosphere, these clusters usually become transformed into closed, denser structures. This could be due to cloud processing as well as water vapor interactions [Hallet *et al.*, 1989]. Particles produced by smoldering combustion in the Pacific Northwest of the United States are nearly spherical and seem to be more stable with respect to aging

[Martins *et al.*, 1996]. No chain aggregates were observed in smoke from the smoldering combustion of biomass (Figures 2f and 2g).

Despite the high variability in particle shapes seen under the SEM, the results from the A^3 suggest that as far as light scattering is concerned, the particles can be approximated by spheres. In all the cases that we analyzed of smoke particles in Brazil, the value of α_0 was less than 13%, with the majority of

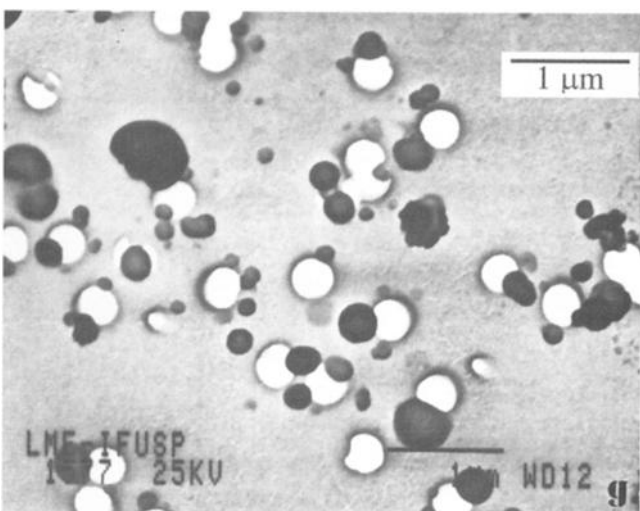
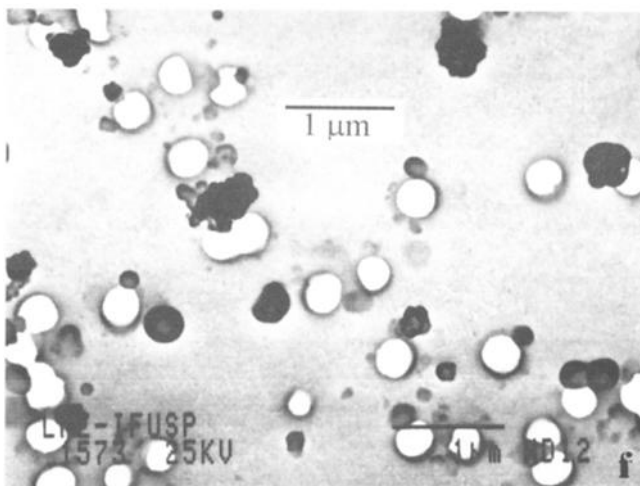
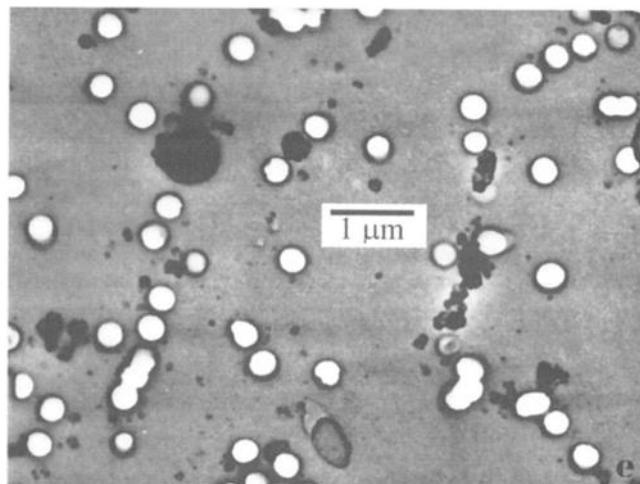


Figure 2. continued

the data (~72% of the cases) below 4%. This indicates the predominance of nearly spherical particles.

Weiss *et al.* [1992] used the same A³ instrument as that used in the present study to measure α_o for the smoke particles from the oil fires in Kuwait in 1991, obtaining α_o values ranging from 4 to 46%. A SEM photograph from a Nuclepore filter exposed in smoke from oil fires in Kuwait is shown in the paper by Weiss *et al.* [1992]; it shows a high concentration of very nonspherical particles in the size range 1 to 4 μm diameter, and relatively few particles with diameters below 0.4 μm (the size range of most of the particles produced by biomass burning in Brazil).

Figure 3 shows α_o as a function of combustion efficiency for the SCAR-B results. Particles from low combustion efficiency fires (CE < 0.9) have an average α_o of about 2%, with values ranging from about 0.5%, for particles collected near Porto Velho, to about 5% for particles collected near Cuiabá. Particles from Cuiabá were likely mixed with soil dust particles, which are larger and nonspherical in general. For high combustion efficiency (CE > 0.9), α_o values range from about 1% up to 11%, with an average value of about 4%. For particles produced by fires with low combustion efficiency, the most nonspherical particles were found in Cuiabá; this could be due to the high concentration of nonspherical soil dust particles at this locale [Artaxo *et al.*, this issue]. The α_o results from Porto Velho show a crescent-shaped curve as a function of CE, clearly associating spherical particles with lower values of combustion efficiency, and highly nonspherical particles with CE values > 0.94.

Figure 4 shows the correlation between the total mass absorption efficiency (α_a) of the particles and α_o . The significant correlation between α_a and α_o shows that higher values of α_a are generally associated with more asymmetrical particles. This can be explained by higher amounts of BC in nonspherical particles than in spherical particles, or by differences in the absorption efficiency due to particle structure [Martins *et al.*, this issue]. Although Martins *et al.* showed that the black carbon mass absorption efficiency (α_{aBC}) varies significantly for biomass burning aerosols, if we assume a constant α_{aBC}

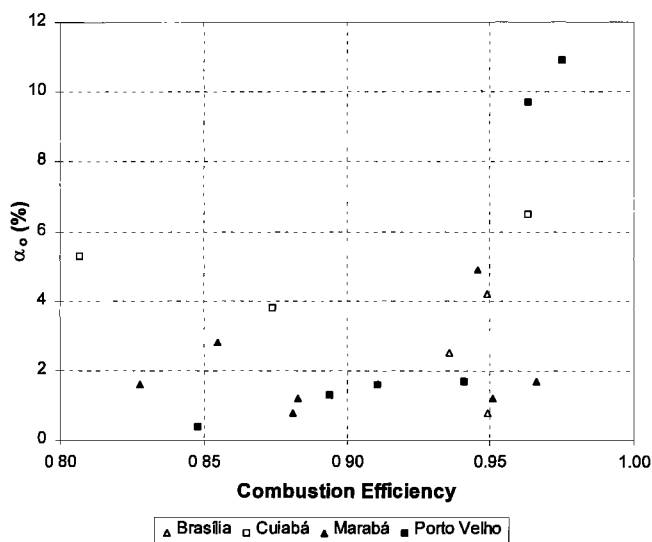


Figure 3. Nonsphericity parameter (α_o) versus combustion efficiency. More asymmetrical particles and clusters are generally associated with higher combustion efficiency (flaming-phase combustion).

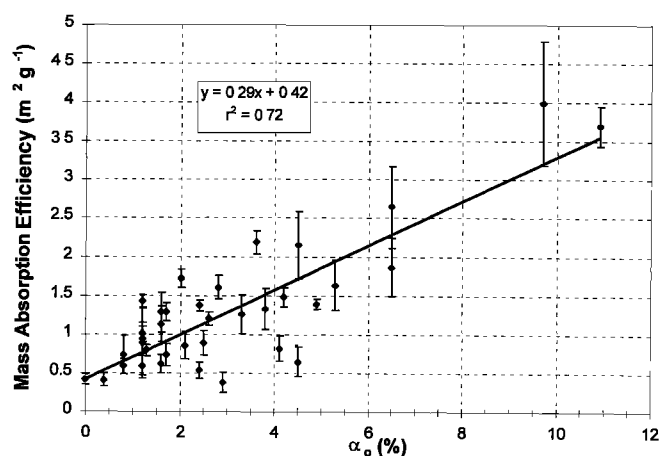


Figure 4. Nonsphericity parameter (α_o) versus the total mass absorption efficiency (α_a). Nonspherical particles and clusters are associated with high values of α_a and high ratios of black carbon (BC) mass to total particle mass (TPM).

value as an example, the fraction BC/TPM is directly proportional to the total mass absorption efficiency shown in Figure 4 [Reid *et al.*, this issue]. This suggests that the nonsphericity of a particle may be proportional to the relative amount of black carbon in the sample. Thus high BC/TPM ratios may be related to nonspherical particles and flaming phase combustion [Lobert and Warnatz, 1993; Yamasoe, 1994; Martins *et al.*, 1996]. Flaming phase combustion may also eject large, asymmetrical soil particles into the atmosphere, contributing to the light absorption and the correlation between α_a and α_o seen in Figure 4. However, there was no evidence for this in the chemical or SEM results for these samples.

3.2. Samples From Regional Hazes

Most of the A³ measurements were made on smoke in individual plumes. However, to assess the climatic effects of the particles, it is important to characterize older smoke particles in regional hazes. While young smoke is composed of spherical and nonspherical particles, depending on the type of combustion and fuel, aged particles in the regional hazes were usually more spherical and compacted. Young smoke particles are subject to quick evolution and aging, which promotes rapid transformations in their structure, size, and composition [Reid and Hobbs, this issue]. The large chain aggregates (a few up to tens of micrometers in size) commonly found in young smoke, and produced by flaming combustion, usually break down and/or collapse into closely packed, submicrometer particles with distinct optical and physical properties as they age [Martins *et al.*, this issue].

Figure 5a shows one of the most extreme cases of nonspherical particle in a regional haze observed in SCAR-B. This sample was collected in aged smoke near cloud base over Cuiabá. The figure shows a combination of spherical and nonspherical particles, with compact aggregates and few small open BC clusters. Figure 5b shows another sample from regional haze over Cuiabá which contain mostly spherical particles. All the samples observed in regional hazes in Cuiabá, Marabá, and Porto Velho ranged between the types of particles shown in Figures 5a and 5b. Comparison of these results with those from the A³ and SEM photographs for young smoke

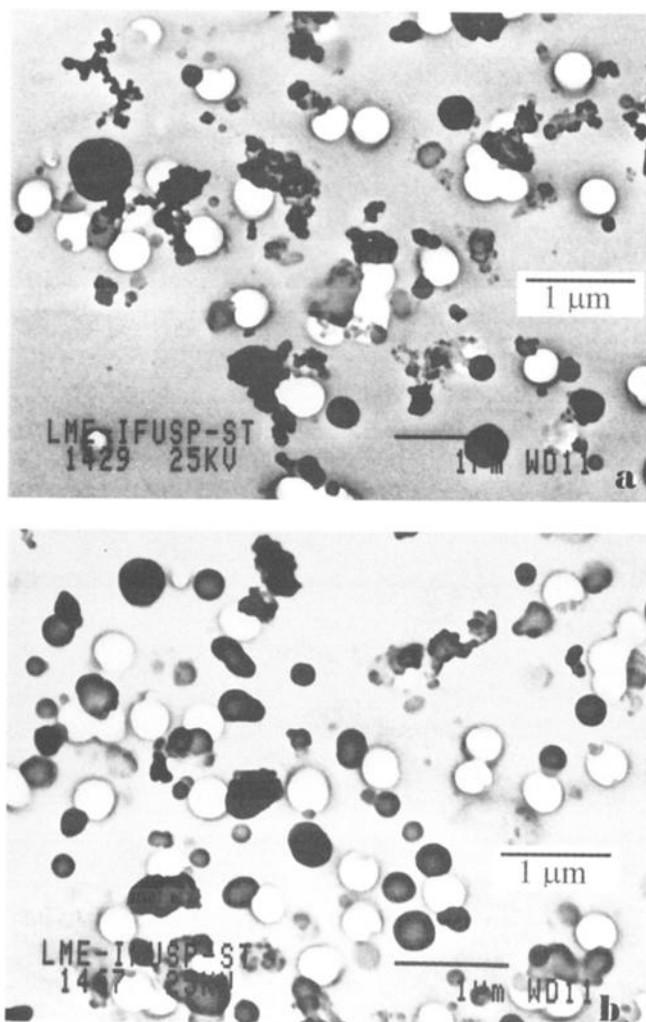


Figure 5. (a) Particles in aged smoke at cloud base collected near Cuiabá. This photograph represents some of the most nonspherical particles collected in regional hazes in SCAR-B. (b) Particles collected at 5000 ft in regional haze over Cuiabá.

particles suggests that the spherical approximation for smoke particles from biomass burning is generally reasonable.

4. Conclusions

Smoke particles from smoldering combustion and aged smoke particles tend to be spherical. Measurements from electrooptical nephelometry and SEM photographs suggest that smoke particles in regional hazes over the Amazon Basin can be approximated by spheres for the purpose of estimating their optical properties. The nonsphericity of smoke particles from biomass burning is correlated with combustion efficiency, with the mass absorption efficiency, and probably with the ratio of black carbon to the total particle mass. High combustion efficiencies (flaming combustion) produce high black carbon contents and particles that are more nonspherical. Most of the nonspherical particles in smoke from biomass burning in Brazil are chain aggregates of small, black carbon particles.

Acknowledgments. The University of Washington's participation in SCAR-B was supported by the following grants: NASA NAGW-3750 and NAG 11709; NSF ATM-9400760, ATM-9412082, and ATM-

9408941; NOAA NA37RJ0198AM09; and EPA CR822077. J. V. Martins and P. Artaxo thanks the Brazilian agencies FAPESP (project 93/5017-3 and 96/2672-9) and CAPES (project 437/95) for financial support. The SEM photographs were taken at the Laboratório de Microscopia Eletrônica, Instituto de Física da USP (University of São Paulo). We thank Alcides C. Ribeiro, Ana L. Loureiro, and Tarsis Germano for assistance during sampling and analysis.

References

- Artaxo, P., E. T. Fernandes, J. V. Martins, M. A. Yamasoe, P. V. Hobbs, W. Maenhaut, K. M. Longo, and A. Castanho, Large-scale aerosol source apportionment in Amazonia, *J. Geophys. Res.*, this issue.
- Cheng, M. T., G. W. Xie, M. Yang, and D. T. Shaw, Experimental characterization of chain-aggregate aerosol by electro-optical scattering, *Aerosol Sci. Technol.*, *14*, 74–78, 1991.
- Chylek, P., and V. Ramaswamy, Lower and upper bounds on extinction cross sections of arbitrarily shaped strongly absorbing or strongly reflecting nonspherical particles, *Appl. Op.*, *21*, 4339–4345, 1982.
- Hallet, J., J. G. Hudson, and C. F. Rogers, Characterization of combustion aerosols for haze and cloud formation, *Aerosol Sci. Technol.*, *10*, 70–83, 1989.
- Hobbs, P. V., J. S. Reid, R. A. Kotchenruther, R. J. Ferek, and R. Weiss, Direct radiative forcing by smoke from biomass burning, *Science*, *275*, 1776–1778, 1997.
- Kahn, R., R. West, D. McDonald, B. Rheingans, and M. I. Mishchenko, Sensitivity of multiangle remote sensing observations to aerosol sphericity, *J. Geophys. Res.*, *102*, 16,861–16,870, 1997.
- Kapustin, V. N., G. V. Rosenberg, N. C. Ahlquist, D. S. Covert, A. P. Waggoner, and R. J. Charlson, Characterization of nonspherical atmospheric aerosol particles with electrooptical nephelometry, *Appl. Op.*, *19*, 1345–1348, 1980.
- Kaufman, Y. J., R. S. Fraser, and R. A. Ferrare, Satellite measurements of large-scale air pollution: Methods, *J. Geophys. Res.*, *95*, 9895–9909, 1990.
- Kaufman, Y. J., and R. S. Fraser, The effect of smoke particles on clouds and climate forcing, *Science*, *277*, 1636–1639, 1997.
- Lober, J. M., and J. Warnatz, Fire in the environment, in *Dahlem Workshop Reports, Environ. Sci. Res. Rep. 13*, edited by P. J. Crutzen and J. G. Goldammer, John Wiley, New York, 1993.
- Martins, J. V., P. Artaxo, P. V. Hobbs, C. Liou, H. Cachier, Y. Kaufman, and A. Plana-Fattori, Particle size distributions, elemental compositions, carbon measurements and optical properties of smoke from biomass burning in the Pacific Northwest of the United States, in *Biomass Burning and Global Change*, edited by J. S. Levine, pp. 716–732, MIT Press, Cambridge, Mass., 1996.
- Martins, J. V., P. Artaxo, C. Liou, J. S. Reid, P. V. Hobbs, and Y. Kaufman, Effects of black carbon content, particle size, and mixing on light absorption by aerosol from biomass burning in Brazil, *J. Geophys. Res.*, this issue.
- Mishchenko, M. I., L. D. Travis, R. A. Kahn, and R. A. West, Modeling phase functions for dustlike tropospheric aerosols using a shape mixture of randomly oriented polydisperse spheroids, *J. Geophys. Res.*, *102*, 16,831–16,847, 1997.
- Mugnai, A., and W. Wiscombe, Scattering from nonspherical Chebyshev particles, I, Cross sections, single-scattering albedo, asymmetry factor, and backscattered fraction, *Appl. Op.*, *25*, 1235–1244, 1986.
- Mugnai, A., and W. Wiscombe, Scattering from nonspherical Chebyshev particles, 3, Variability in angular scattering patterns, *Appl. Op.*, *28*, 3061–3073, 1989.
- Penner, J. E., R. Dickinson, and C. O'Neil, Effects of aerosol from biomass burning on the global radiation budget, *Science*, *256*, 1432–1434, 1992.
- Reid, J. S., and P. V. Hobbs, Physical and optical properties of young smoke from individual biomass fires in Brazil, *J. Geophys. Res.*, this issue.
- Reid, J. S., P. V. Hobbs, C. Liou, J. V. Martins, R. E. Weiss, and T. F. Eck, Comparisons of techniques for measuring shortwave absorption and black carbon content of biomass burning aerosols, *J. Geophys. Res.*, this issue.
- Ward, D. E., R. A. Susott, J. B. Kauffman, R. E. Babbitt, D. L. Cummings, B. Dias, B. N. Holben, Y. J. Kaufman, R. A. Rasmussen, and A. W. Setzer, Smoke and fire characteristics for cerrado and deforestation burns in Brazil: Base-B experiment, *J. Geophys. Res.*, *97*, 14,601–14,619, 1992.

- Weiss, R. E., V. N. Kapustin, and P. V. Hobbs, Chain-aggregate aerosols in smoke from the Kuwait oil fires, *J. Geophys. Res.*, *97*, 14,527–14,531, 1992.
- West, R. A., L. R. Doose, A. M. Eibl, M. G. Tomasko, and M. I. Mishchenko, Laboratory measurements of mineral dust scattering phase function and linear polarization, *J. Geophys. Res.*, *102*, 16,871–16,881, 1997.
- Wiscombe, W. J., and G. W. Grams, The backscattered fraction in two-stream approximations, *J. Atmos. Sci.*, *33*, 2440–2451, 1976.
- Wiscombe, W., and A. Mugnai, Scattering from nonspherical Chebyshev particles, 2, Means of angular scattering patterns, *Appl. Op.*, *27*, 2405–2421, 1988.
- Yamasoe, M. A., Estudo da composicao elementar e ionica de aerossóis emitidos em queimadas na Amazonia (in Portuguese), M.S. thesis, Univ. of Sao Paulo, Brazil, 1994.
-
- P. Artaxo and J. V. Martins, Instituto de Física, Universidade de São Paulo, C. Postal 66318, CEP 05315-970, São Paulo, Brazil. (e-mail: vanderlei@if.usp.br)
- P. V. Hobbs, Department of Atmospheric Sciences, University of Washington, Seattle, WA 98195-1640.
- R. E. Weiss, Radiance Research, Inc., Seattle, WA 98177.

(Received October 6, 1997; revised March 16, 1998;
accepted March 18, 1998.)